CAMBRIDGE UNIVERSITY PRESS

RESEARCH ARTICLE

Dynamics of turbulence in the field of nonlinear internal waves

Lev A. Ostrovsky^{1,2,3} , Irina Soustova³ and Alexandra Kuznetsova^{3,4}

Corresponding author: Lev A. Ostrovsky; Email: lev.ostrovsky@gmail.com

Keywords: density fluctuations; Gardner soliton; internal gravity waves; internal soliton; pycnocline

(Received 2 June 2025; revised 12 August 2025; accepted 23 August 2025)

Abstract

A modification of the semi-empirical theory of stratified turbulent flow, which includes an equation for the density fluctuations (the potential energy of turbulence), is applied to describe the effect of internal gravity waves (IWs) on the small-scale turbulence. After considering the periodic IWs, special attention is paid to the action of internal solitons, such as the classical Gardner solitons and a strongly nonlinear solitary wave regularly observed in the Oregon Bay of the USA. It is confirmed that the presence of potential energy allows the existence of finite turbulence at any Richardson number.

1. Introduction

Internal solitons in the ocean (ISWs) are, arguably, the most commonly observed kind of solitary waves (or structures close to them) in nature. Despite a relatively long history of such observations, many related theoretical problems remain unsolved. It refers, among others, to strongly nonlinear solitons that cannot be described by the classical Korteweg-de Vries equation and its numerous modifications. Strongly nonlinear solitons are rather common in the ocean, particularly on oceanic shelves where they are generated by the barotropic tide. There are many works on the observation and description of solitonlike waves in the shelf regions [1-7]. An even more complex factor is that in the oceanic conditions, internal solitons always interact with other motions of different scales, including currents, turbulence and surface waves. All that contributes to the 'internal weather' and, in particular, to the dynamics of biological components and impurities responsible for the ecological environment. Here we limit ourselves to one, albeit broad, class of processes: the interactions between internal waves (IWs) and small-scale turbulence. This, in turn, can be conditionally broken into several problems. The one is the attenuation of internal waves due to turbulent viscosity and diffusion [8-11]. Another is how internal waves generate turbulence, which is observed almost everywhere in the ocean, including its deep areas. It is often associated with shear instability that, according to the classical Miles-Howard theory, is possible if $Ri < \frac{1}{4}$, where Ri is the Richardson number [12, 13], and the eventual generation of turbulence. At the same time, turbulence is regularly observed for larger values of Ri. For a developed turbulence when the semi-empirical description is valid, the turbulence can be maintained under a softer condition, Ri < 1. However, in many cases, turbulence exists at Ri > 1, i.e., for a much stronger stratification [14–19]. The explanation of that is based on a modification of the classical semi-empirical theory of turbulence suggested in Ostrovsky and Troitskaya [20], where the kinetic equation for the distribution function of

© The Author(s), 2025. Published by Cambridge University Press. This is an Open Access article, distributed under the terms of the Creative Commons Attribution licence (http://creativecommons.org/licenses/by/4.0), which permits unrestricted re-use, distribution and reproduction, provided the original article is properly cited.

¹University of Colorado, Boulder, CO, USA

²University of North Carolina, Chapel Hill, NC, USA

³A.V. Gaponov-Grekhov Institute of the Applied Physics of the Russian Academy of Sciences, Nizhny Novgorod, Russian Federation

⁴National Research University Higher School of Economics, Nizhny Novgorod, Russian Federation

velocity and density fluctuations was used. This approach reduces the number of arbitrary constants in the semi-empirical equations and, more importantly, it adds an equation for the potential energy of turbulence, which is proportional to the variance of density fluctuations. As a result, the restriction on the value of *Ri* can be completely removed so that turbulence energy can remain finite at any finite velocity shear. The application of this theory to the turbulence dynamics under the action of shear flow in different areas of the ocean was studied in refs [20–24]. The case of internal waves is similar but more complicated because the results depend not only on the IW amplitude but also on the ratio between the time scales of the wave and those of generation and relaxation of turbulent energy. There exists extensive literature regarding turbulence generation by instability and breaking of internal waves (e.g. [25–27], and references therein). Here we are interested in the effect of non-breaking IW supporting turbulence long after a breaking event. This effect was observed in the laboratory experiment [28], where a standing internal wave amplified turbulence penetrating downwards from a vibrating perforated grid. For the oceanic observations, we discuss below the effect of strong internal solitons on turbulence at large Richardson numbers.

Theoretical descriptions of stratified turbulence and the corresponding numerical modeling methods, besides the classical semi-empirical (gradient) schemes (RANS), use Large Eddy Simulation (LES) and direct numerical simulation (DNS). The difference between these schemes is based on the degree of resolution of turbulent pulsations and their energy spectrum. Over the past 30 years, new approaches have been developed to study the characteristics of stratified turbulence based on the spectral approach (e.g [29]). These models potentially allow for a more consistent description of the unsteady processes of interaction between turbulence and internal waves than RANS models. More references can be found in Gladskikh et al. [23]. For the problems considered here, we refer to the direct numerical simulation of the IW action on turbulence [30].

Returning to the theme of this paper, we consider the model mentioned above, where the given mean fluid velocity field $\mathbf{u}(\mathbf{r}, t)$ depends on time due to an internal wave. In these cases, the general equations derived in [20] (see also [21, 23]) are reduced to the equations for the turbulent kinetic energy (TKE, K) and turbulent potential energy (P) in the form [8, 20]:

$$\frac{\partial K}{\partial t} + (\mathbf{u}\nabla) K = L\sqrt{K} \left(\frac{\partial u_i}{\partial x_k} + \frac{\partial u_k}{\partial x_i} \right)^2 - N^2 L\sqrt{K} \left[1 - \frac{3P}{K} (1 - G) \right] - \frac{CK^{3/2}}{L} + \frac{5}{3} \frac{\partial}{\partial x_i} \left(L\sqrt{K} \frac{\partial K}{\partial x_i} \right),$$

$$\frac{\partial P}{\partial t} + (\mathbf{u}\nabla) P = N^2 L\sqrt{K} \left[1 - \frac{3P}{K} (1 - G) \right] - \frac{DK^{1/2}}{L} P + \frac{\partial}{\partial x_i} \left(\frac{L\sqrt{K}}{\rho N^2} \frac{\partial (\rho N^2 P)}{\partial x_i} \right). \tag{1}$$

Here, $N^2(z) = (g/\rho)d\rho/dz$ is the squared Brunt-Vaisala (buoyancy) frequency, \mathbf{g} is the gravity acceleration, and $\rho(z)$ is the mean density. C and D are empirical constants (in what follows, they are taken C = D = 0.09), L is the outer scale of turbulence, and G is the anisotropy parameter, which depends on the ratio $s = \frac{L_z}{L_x}$ of the vertical to horizontal correlation scales of turbulence. As shown in Ostrovsky and Troitskaya [20], if $s \ll 1$ (strongly anisotropic "pancake" turbulence), then G is close to 1, and the common gradient theory, neglecting potential energy, is valid. In the quasi-isotropic case, typical of small-scale turbulence, s is close to 1 and s0 significantly differs from 1, so that equations (1) must be solved together. Here, S1 is taken.

2. Turbulence affected by a periodic IW

Some characteristic features of the process can be elucidated from considering the effect of a sinusoidal (linear or weakly nonlinear) internal wave mode; note that equations (1) for turbulence remain nonlinear. A single IW mode with the velocity components $u_z = W$, $u_x = U$ for such waves has the form

$$W = A\sin(k_z z)\cos(\omega t - k_x x), \ U = A(k_z/k_x)\cos(k_z z)\sin(\omega t - k_x x). \tag{2}$$

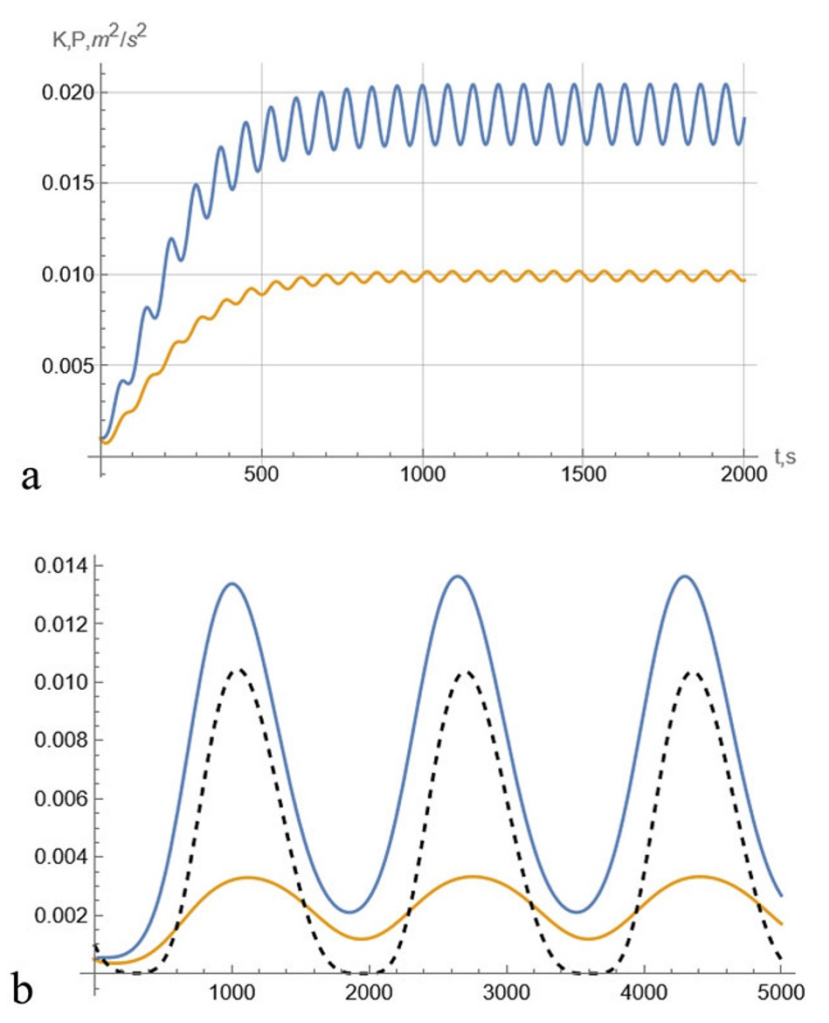


Figure 1. Effect of the internal waves of different frequencies on a turbulent layer in a given vertical cross-section (x = 0). Parameters in (2) are x = 0, and z = 5 m, L = 1. (a) A = 0.02 m/s, ω = 0.04 rad/s, N = 0.049 rad/s; (b) A = 0.01 m/s, ω = 0.0019 rad/s, N = 0.01645 rad/s. Blue: kinetic, orange: potential energy. The dashed line in the bottom plot is for the classic model without potential energy (only the first equation (1) with G = 1).

Figure 1 shows two cases, both with the last terms responsible for diffusion neglected in (1). Here, equations (2) are local, and the depth z enters as a parameter.

Figure 1 illustrates two qualitatively different kinds of turbulence evolution. For a high-frequency internal wave, the turbulent energy reaches a constant level with relatively small oscillations at a frequency 2ω around it. For a longer wave, turbulence energy follows the wave energy. Note that within the classical theory, such a process, among others, was briefly considered by Ivanov et al. [31]. In that case, the turbulence level can drop to practically zero (dashed line in the bottom plot) when the semi-empirical approach becomes inapplicable. In the system (1), where the turbulent potential energy is significant, such an effect is less pronounced, as there is no critical level of Ri.

The above results are valid if the vertical scale of the wave mode is large (small k_z). Otherwise, the diffusion terms in (1) are important. Figure 2 illustrates their effect.

In these cases, the saturation of the energy level occurs more slowly, and in the high-frequency case (a), an additional modulation with a period of about 4000 remains.

4 Ostrovsky et al.

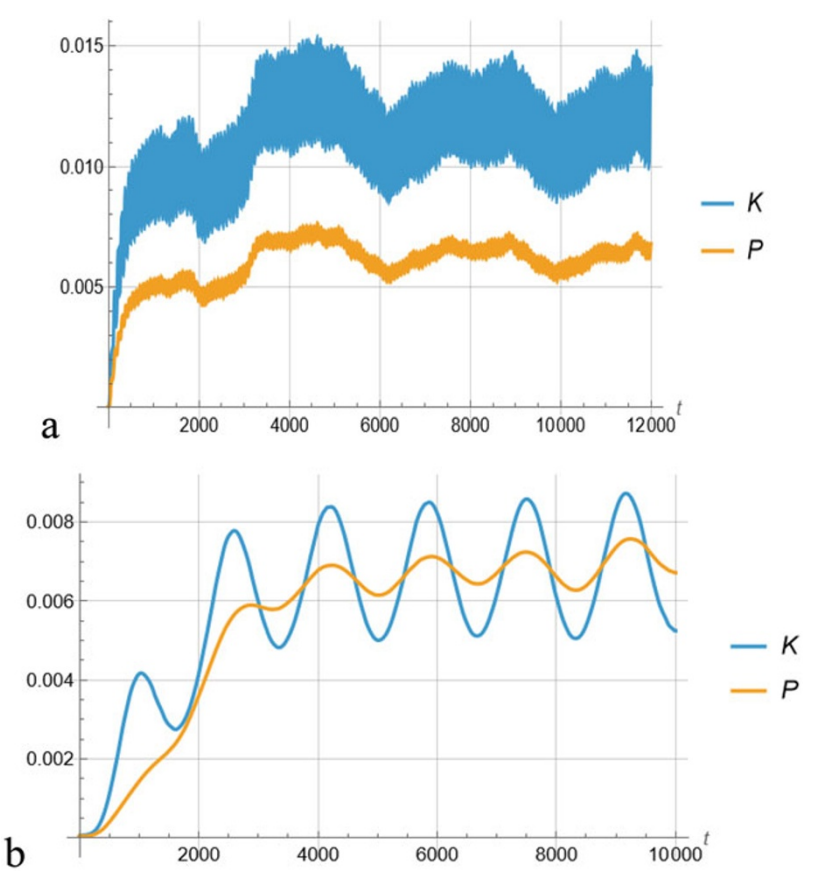


Figure 2. Evolution of turbulent energies with the diffusion effect. The parameters are the same as in Figure 1, at $k_z = 10k_x = 0.1\pi$. They correspond to the cases (a) and (b) in Figure 1.

3. Effect of solitons

3. 1. The post-soliton stage

The action of localized internal waves, including solitary waves, on turbulence depends on the relationship between the duration of the soliton and the characteristic time of turbulence variation, so that it may either follow the wave profile in a quasi-stationary way or react with a delay. Rather universal is the turbulence decay after the soliton impact, when $\mathbf{u} = 0$. Due to the Kolmogorov-type dissipation, the values of K and P become small. At this stage, the last two terms in both equations (1) are of the order of $K^{3/2}$, whereas the terms with N^2 are of the order of $K^{1/2}$. Hence, asymptotically, the terms with N^2 would dominate. Since these terms have opposite signs for positive K and P, the two equations (1) can be compatible only if these terms go to zero. As a result, asymptotically we have

$$3P = K/(1-G), G \neq 1.$$
 (3)

If (3) is met, equations (1) are separated, and the solution for K at $K(t_0) = K_0$ is

$$K(t \ge t_0) = \frac{K_0}{\left[1 + C\sqrt{K_0}(t - t_0)/2L\right]^2}.$$
 (4)

As will be seen below, these simple relations can be true even shortly after the soliton.

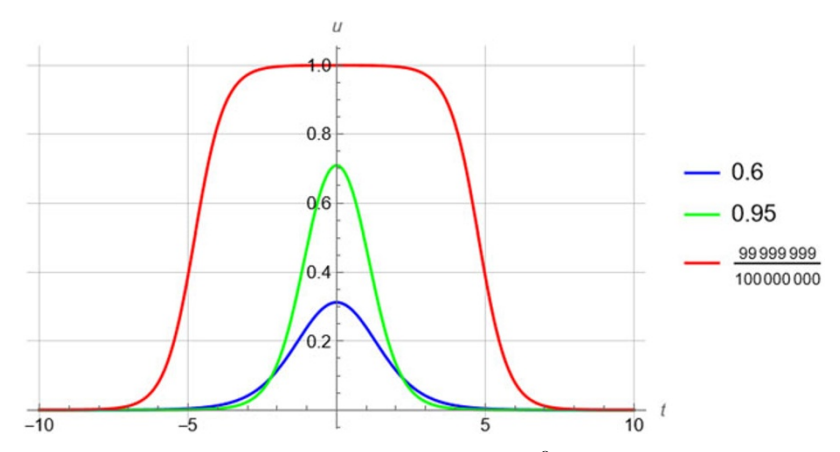


Figure 3. The solitons (6) for k = 0.6, 0.95, and $1-10^{-8}$ (from the smaller to the larger).

3.2. The effect of Gardner solitons

As the first example, consider the action of solitons, which are the solutions of the classic Gardner equation (e.g. [1]). The vertical shear of the horizontal fluid velocity in a wave mode corresponding to (1) has the form $u_z = U(t, x) f_z(z)$. In the dimensionless variables, the factor U satisfies the equation

$$U_t + U_x + 6(U - U^2)U_x + U_{xxx} = 0. (5)$$

Here (5) is written in the original variables x and t, adding the velocity of a long linear wave, $c_0 = 1$. In physics, the corresponding equation is still weakly nonlinear, but unlike the KdV solitons, its solitary solutions can broaden with amplitude, up to its limiting value when the soliton becomes flat-top. This is also characteristic of strongly nonlinear solitons [1, 2]. The solitary solutions of (5) are [1]:

$$U = \frac{k}{2} \left[\tanh \frac{k}{2} \left(x - t - k^2 t + \Delta \right) - \tanh \frac{k}{2} \left(x - t - k^2 t - \Delta \right) \right],$$

$$\Delta = k^{-1} \operatorname{arctanh}(k), \ 0 \le k \le 1.$$
(6)

At small k, this solution is close to the KdV soliton, whereas near k = 1, it defines a flat-top soliton. The examples are plotted in Figure 3.

Consider first the local, non-diffusive model. In eqs. (1), we let $N^2 = 0.25$ and $(df/dz)^2 = 0.2$ at a given level of z. The local Richardson number is $Ri = N^2/u_z^2 = 1.25/U^2$. Figure 4 shows the time dependence of Ri for three values of the parameter k in (6). It exceeds unity for all times, so that the classic gradient model would prevent any support of turbulence by such a wave.

The corresponding solutions of equations (1) are shown in Figure 5. As in the previous section, the local, non-diffusive model is valid if the vertical scale of the velocity field is sufficiently large. The diffusive case was calculated for a mode proportional to $\cos(k_z z)$ with $k_z = 0.1\pi$, as in the case of a sinusoidal wave.

Again, because of the effect of potential energy, turbulence exists at all Richardson numbers. Note that, in agreement with (3), here K = 1.5 P for, roughly, $t \ge 10$. The inertial character of the process is evident, and the solutions (3) and (4) are valid almost immediately after the soliton. Figure 6 shows a 3D plot showing the space-time behavior of the kinetic energy of turbulence under the action of a flat-top soliton.

Note that, in this case, the diffusive terms in eqs. (1) significantly diminish the level of turbulent energy.

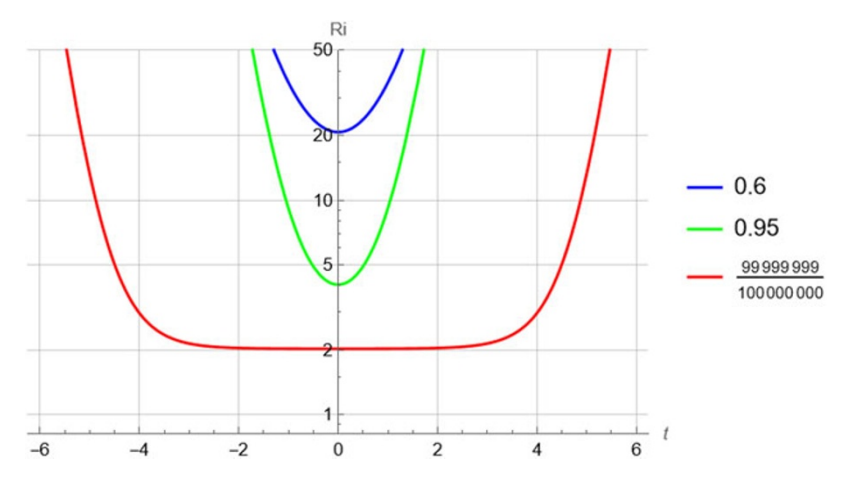


Figure 4. Variation of local Richardson number for the solitons shown in *Figure 3*, with the same values of k.

3.3. Effect of strong internal solitons on turbulence in the ocean

Applications to real field data in the ocean and the atmosphere are more complicated due to the simultaneous action of different uncontrolled factors. As a result, the available publications rarely present sufficient quantitative data to be used in the theory. Here the model (1) is applied to the oceanic data described by Moum et al. [14], where the effect of strongly nonlinear internal solitons on small-scale turbulence was observed off the North-Western Pacific coast of the USA. Even though rather scarce quantitative data are given, the figures illustrating the effect allow us to make reasonable estimates. Some preliminary results have been illustrated in our short presentation [24]. Note also that some topics of the present paper have been briefly outlined in the review paper of one of the authors published earlier [11] with a reference to this paper as being prepared. Here we further study this problem.

For the time dependence of soliton parameters, we use the echosounder images of the leading soliton in the observed group shown in several figures of [14]. In its Figure 7, the plots are supplemented by isolines of density (isopycnals), color images of fluid velocity, and turbulent kinetic energy dissipation rate. The latter is a commonly measured turbulence characteristic in the ocean, and where possible, we shall verify theoretical results by comparison with the data of the turbulent dissipation rate.

Figure 7 here shows the time profile of the leading solitary wave in the group.

Note that the corresponding isopycnal is depressed from about 10 m to about 36 m, which testifies to a very strong nonlinearity. Moreover, according to Figure 2 of [14], the total water depth in the observation area is 100 m or slightly more. Therefore, the wave moves down a significant part of the total water layer.

3.4. Quasistatic approximation

Consider first the quasi-static approximation, supposing that the soliton duration is longer than the time needed for saturation of the turbulence parameters. For the field experiment (Figure 15 of [14]), vertical profiles of horizontal velocity and density are shown for a vertical cross-section marked by the dot in Figure 7. We digitized and interpolated these profiles, as shown in Figure 8. The motion of the density jump (here at about 30 m depth) seen in Figure 8b will be considered further in the paper.

As mentioned in Moum et al. [14], the data for fluid velocity obtained from ADCP is rough, so further averaging is justified. Then, we found the depth dependence of the functions $(du/dz)^2$ and N^2 entering the system (1), where u is the horizontal velocity. Their variation in depth is shown in Figure 9.

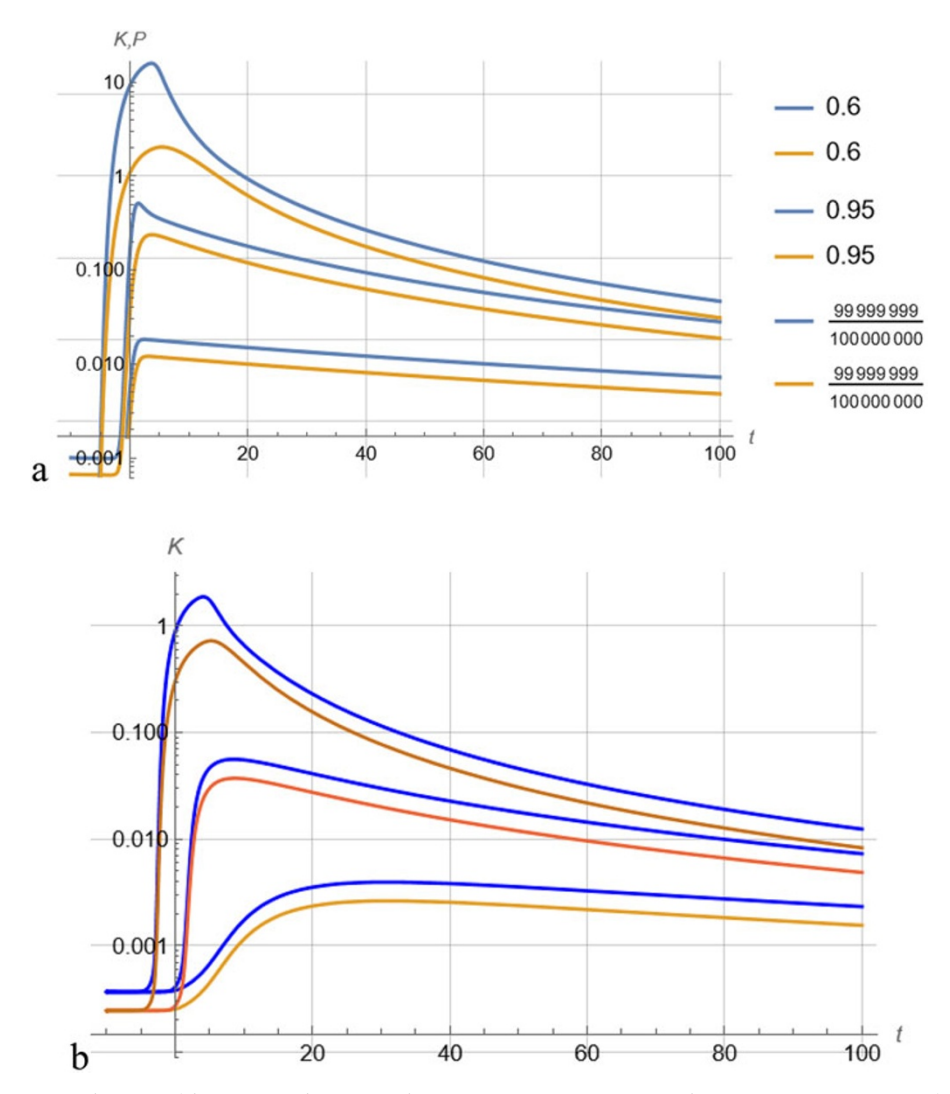


Figure 5. Evolution of kinetic and potential energies at z = 5. From lower to upper pairs of curves: k = 0.6, 0.95, and $1-10^{-8}$. Blue-kinetic, maroon-potential energy of turbulence. (a) Without diffusion, (b) with diffusion.

Figure 10 shows the resulting profile of the Richardson number $Ri = N^2/(du/dz)^2$. For almost all depths considered (from 15 to 42 m), Ri > 1, and again, the turbulence can be supported by the wave only because of the effect of its potential energy.

Substituting $(du/dz)^2$ and N^2 as functions of z into (1), we obtain the depth dependence of kinetic and potential energies as shown in Figure 11. Figure 12 shows the corresponding distribution of the TKE dissipation rate $\varepsilon = CK^{3/2}/L$, which is a rather common value measured in oceanic experiments as a characteristic of turbulence level [14, 15].

3.5. Non-stationary processes

The above results qualitatively correspond to the data of [14]. Indeed, the turbulence level has two maxima, one near the water surface (supposedly because of wind wave breaking), another at a depth of about 38 m, not far from the experimental data. However, there are some discrepancies. In particular,

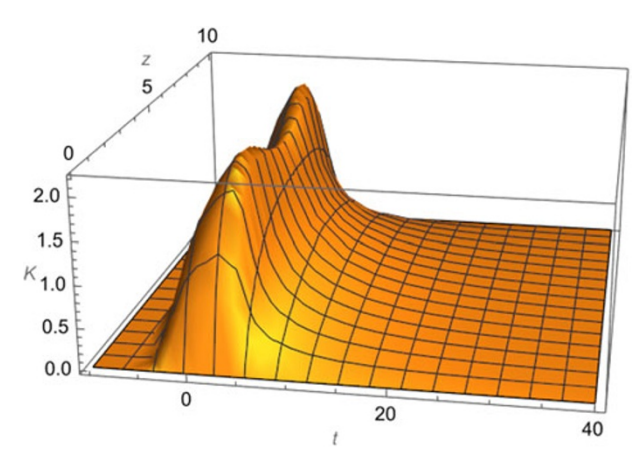


Figure 6. 3D plot of kinetic turbulent energy for $k = 1-10^{-8}$.

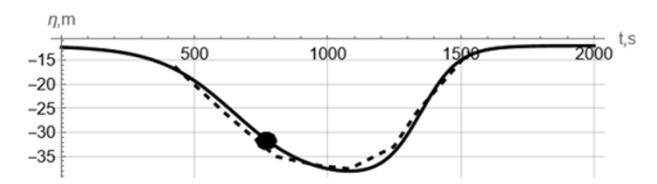


Figure 7. Time profile of the leading soliton, digitized (dashed) and interpolated (solid) from the echosounder image shown in [14]. The black dot marked in Figure 9 of that paper shows the approximate position of the contact device, measuring the wave vertical profile as shown in their Figure 15.

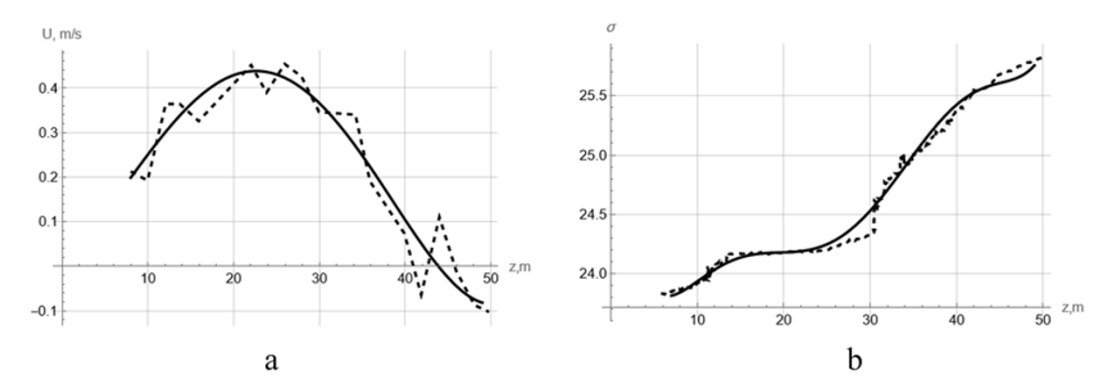


Figure 8. Depth dependencies of horizontal velocity u (left) and normalized excess density $\sigma = (\rho - \rho_0)/\rho_0$ (right). Here it is taken $\rho_0 = 1000 \text{ kg/m}^3$. Dashed lines: digitized plots of those in [14]. Solid lines: their polynomial interpolations.

the TKE dissipation rate (about 5.10^{-5} m²/s³) exceeds by about an order the data of the cited paper indicated by a color bar in its Figure 6. To evaluate the applicability of the quasistatic approach, we considered a transient process by solving non-stationary equations (1) for the same data as those used above. One result is shown in Figure 13.

Figure 14 shows the corresponding variation of dissipation rate.

As seen from these figures, the transient process takes about 10–15 min, which is comparable to the duration of the soliton shown in Figure 7. Therefore, to determine the dynamics of turbulence in the field of a strongly nonlinear soliton of internal waves, it is necessary to take into account the time

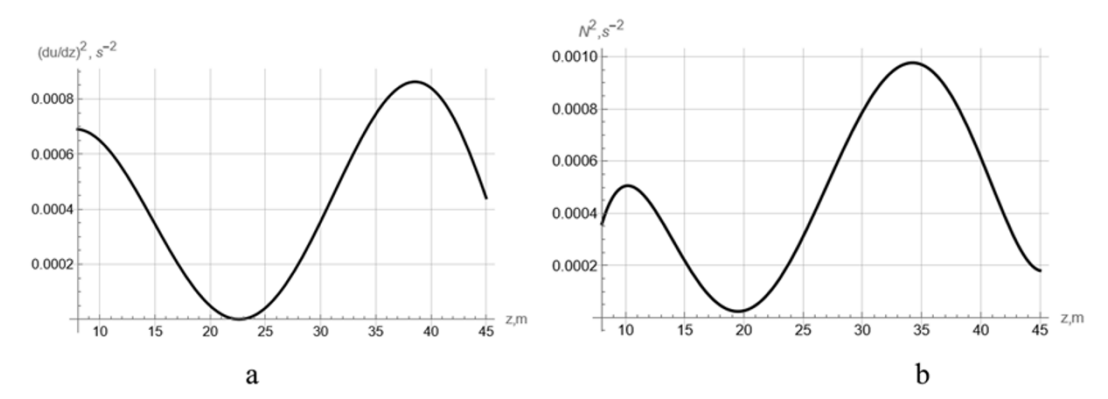


Figure 9. Interpolated depth dependencies of functions $(du/dz)^2$ (a) and N^2 (b). Here, u is the horizontal component of fluid velocity (for a long wave considered here, the vertical velocity variation can be neglected in this context).

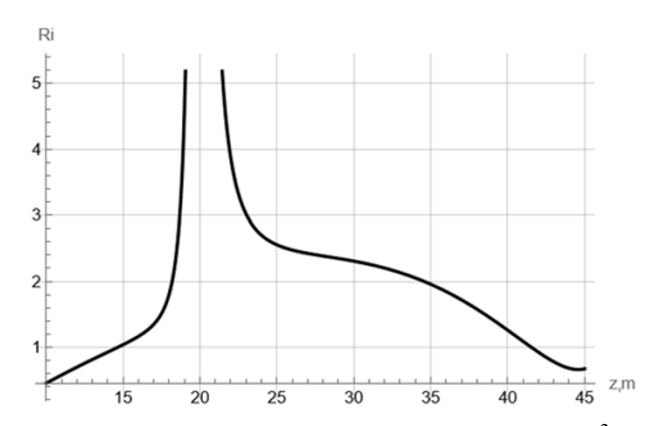


Figure 10. Depth dependence of Richardson number $Ri = N^2/(du/dz)^2$.

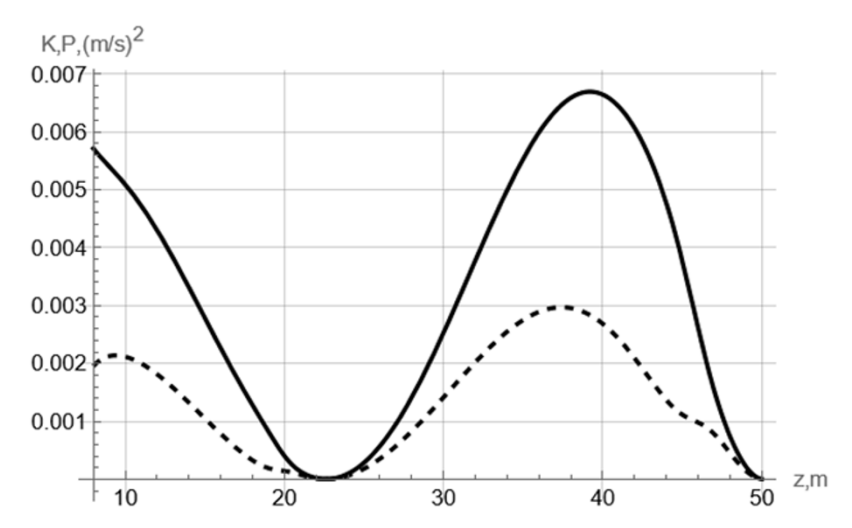


Figure 11. Depth dependence of kinetic (solid line) and potential (dashed line) energies in the quasistatic approximation, L = I m.

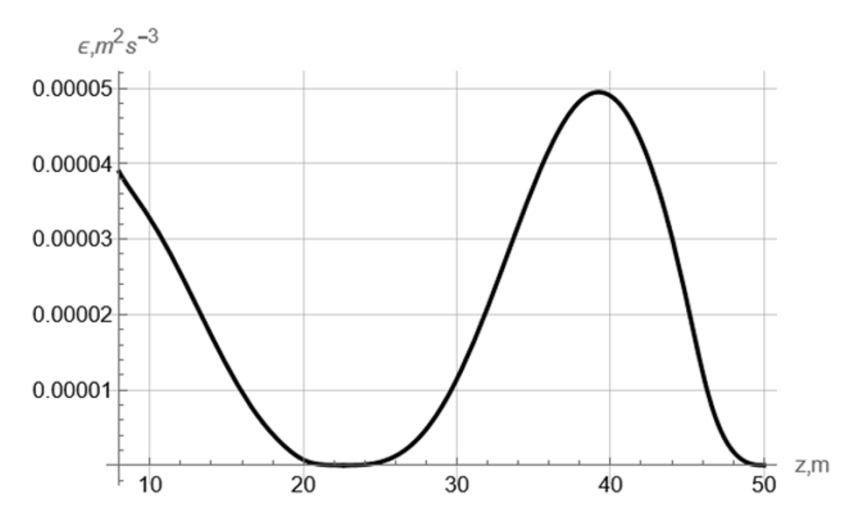


Figure 12. Depth dependence of TKE dissipation rate in the quasistatic approximation.

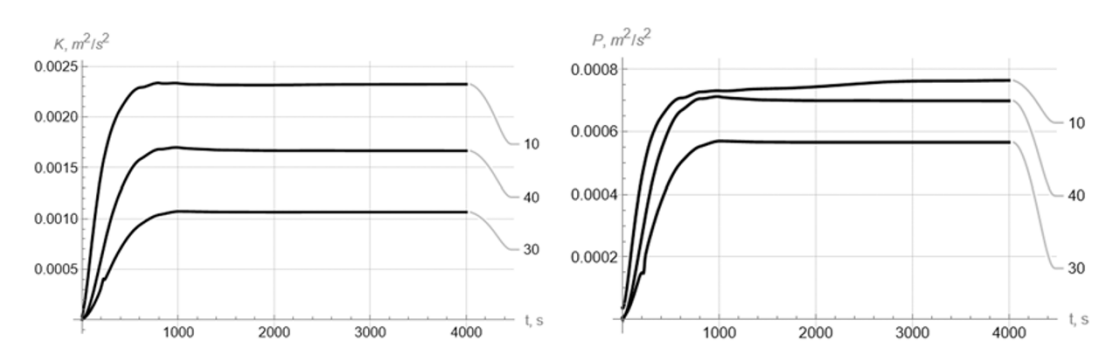


Figure 13. Growth of turbulent kinetic (left) and potential (right) energies from small initial values to saturation at three depths, 10, 30, and 40 m.

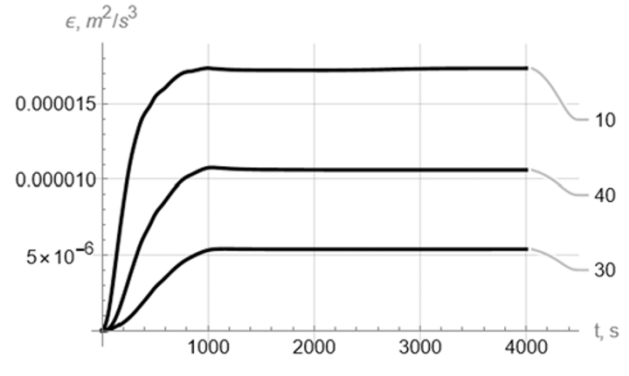


Figure 14. Growth of the turbulence dissipation rate at different depths.

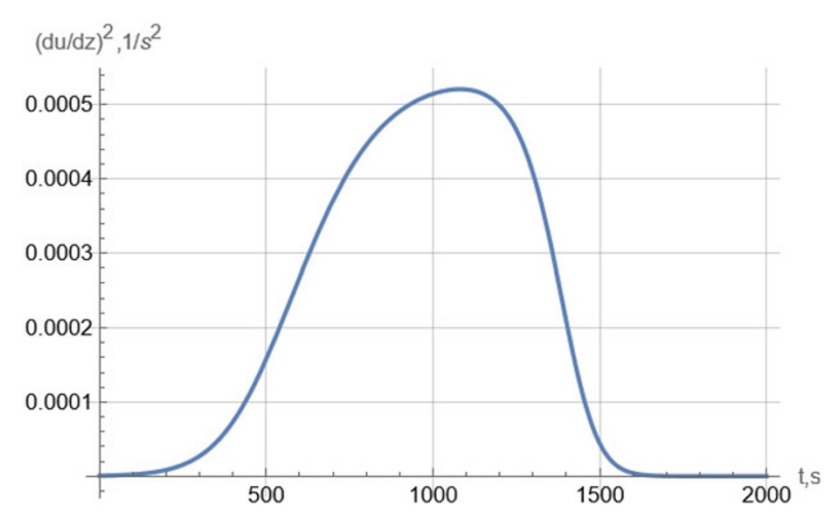


Figure 15. Variation of squared vertical shear of the horizontal fluid velocity.

dependence of the squared horizontal velocity shear $\left(\frac{\partial u}{\partial z}\right)^2$ and the squared Brunt–Vaisala frequency N^2 , which are present in system (1).

3.6. Dynamics of turbulence in the pycnocline

To describe the variation of the parameters $\left(\frac{\partial u}{\partial z}\right)^2$ and N^2 at the pycnocline, we begin with the data shown in Figure 8. As mentioned above, there is a density jump at a depth of 30 m in the density profile (Figure 8, dashed line), where the turbulence is concentrated, as seen from the color scattering images shown in [14]. According to Figures 6 and 15 of [14], the velocity u_1 over the pycnocline is almost independent of depth, except for the near-surface area. To find it, we use a relation between u_1 and the pycnocline displacement in a strong soliton given in [2]:

$$u_1 = \frac{c(\eta - h_1)}{\eta}. (7)$$

Here, c is the wave velocity (0.6 m/s in this case), h_1 is the thickness of the upper layer (10–12 m in the experiment [14]) over the pycnocline, and η is the local depth of the pycnocline (this notation is slightly different from that in [2], which is due to the choice of the starting point for depth measurements). The temporal profile of the leading soliton $\eta(t)$ is shown in Figure 7 above. To determine the dependence of the horizontal velocity on time, we assume that the stratification remains unchanged in the pycnocline at the soliton length (about 300 m), and equal to $N^2 = 0.0008$ s⁻². For this purpose, the soliton-like displacement of the pycnocline shown in Figure 7 was approximated as:

$$\eta = -12 + (14 \text{Tanh} [0.007 (t - 350)] - 14 \text{Tanh} [0.0035 (t + 350)]) \text{ m.}$$
 (8)

Using (7), we obtain the time dependence of $\left(\frac{\partial u}{\partial z}\right)^2$ at the pycnocline in the form

$$\left(\frac{\partial u}{\partial z}\right)^2 = \frac{(1.1.10^{-3}(14\,\text{Tanh}[0.007(t-350)] - 14\,\text{Tanh}[0.0035(t+350)])^2}{(1.1.10^{-3}(14\,\text{Tanh}[0.007(t-350)] - 14\,\text{Tanh}[0.0035(t+350)])^2}\,\text{s}^{-2}.\tag{9}$$

It is shown in Figure 15.

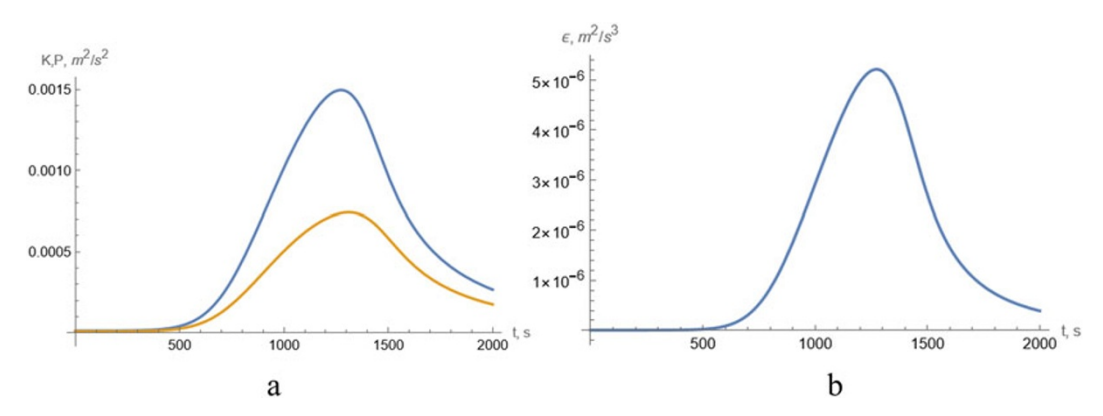


Figure 16. (a) The kinetic (blue) and potential (yellow) turbulent energy densities at the thermocline. (b) TKE dissipation rate variation along the soliton.

The obtained values of N^2 and $\left(\frac{\partial u}{\partial z}\right)^2$ are substituted into the local equations for K and P since the diffusion terms are more than three orders of magnitude smaller than the other terms in (1).

Then, using equations (1), the kinetic and potential energies (Figure 16a) and the kinetic energy dissipation rate (Figure 16b) are calculated.

The obtained results have good agreement with the data of [14], particularly with its Figure 7. First, the order of calculated maximum dissipation rate is about 5.10^{-6} m²/s², which corresponds to the maximum values shown in the color bar in Figure 7 of [14]. Note that the level of dissipation rate before the soliton in the same figure, which can roughly be taken for background, is two orders smaller than that. Second, due to the delay of turbulence development, the maximums of energy and dissipation rate are shifted towards the rear part of the soliton, which also agrees with the sound scattering intensity distribution shown in [14].

Note that the authors of [14] explain the existence of turbulence by the presence of microstructure with a presumably small Richardson number, Ri < 1/4. However, as shown here, the observed values and distributions of turbulent energy can be supported by the IW even at Richardson numbers significantly exceeding unity.

4. Conclusions

The modification of the Reynolds-type equations for turbulence described above was suggested as early as 1987. However, its applications to the observed processes in the stratified flows began only recently [21–24]. Here, the effects of the internal waves, particularly internal solitons, have been considered. It is confirmed that the finite-energy turbulence can exist at large Reynolds numbers (strong stratification), and for a strong internal soliton, the theoretical estimates agree with the observational data, both qualitatively and by order of magnitude. This also helps to explain the ubiquitous presence of turbulence in the ocean. Indeed, even when turbulence is generated by wave breaking events, its long-time existence can be due to the support by non-breaking waves which are more common in most areas of the ocean.

Among the promising future developments, there is the description of the mutual action of internal solitons and turbulence when a soliton dissipates during interaction. Attenuation of internal waves on turbulence was studied in detail for sinusoidal internal waves, see a brief review of that in [11]. For these processes, the variation of turbulence scales in time can be important [32]. This work is in progress.

Acknowledgements. The work was supported by the RSF project No. 23-27-00002. I.A.S. and A. M. K. acknowledge the state assignment of the IAP RAS on the topic FFUF-2025-0026.

The authors are grateful to D.S. Gladskikh for valuable discussions.

References

- Apel JR, Ostrovsky LA, Stepanyants YA and Lynch JF (2007) Internal solitons in the ocean and their effect on underwater sound. The Journal of the Acoustical Society of America 121(2), 695–722. doi:10.1121/1.2395914
- [2] Ostrovsky LA and Grue J (2003) Evolution equations for strongly nonlinear internal waves. *Physics of Fluids* 15(10), 2934–2948. doi:10.1063/1.1604133
- [3] Kropfli RA, Ostrovski LA, Stanton TP, Skirta EA, Keane AN and Irisov V (1999) Relationships between strong internal waves in the coastal zone and their radar and radiometric signatures. *Journal of Geophysical Research: Oceans* 104(C2), 3133–3148. doi:10.1029/98JC02549
- [4] Stanton TP and Ostrovsky LA (1998) Observations of highly nonlinear internal solitons over the continental shelf. Geophysical Research Letters 25(14), 2695–2698. doi:10.1029/98GL01772
- [5] Jackson CR, Da Silva JC and Jeans G (2012) The generation of nonlinear internal waves. *Oceanography* 25(2), 108–123. doi:10.5670/oceanog.2012.46
- [6] Klymak JM and Moum JN (2003) Internal solitary waves of elevation advancing on a shoaling shelf. Geophysical Research Letters 30(20), 2045. doi:10.1029/2003GL017706
- [7] Orr MH and Mignerey PC (2003) Nonlinear internal waves in the South China Sea: observation of the conversion of depression internal waves to elevation internal waves. *Journal of Geophysical Research: Oceans* 108(C3), 3064. doi:10. 1029/2001JC001163
- [8] Monin AS and Yaglom AM (1975) Statistical Fluid Mechanics, Mechanics of Turbulence II, Mineola, New York: DOVER PUBLICATIONS, INC. 882.
- [9] **LeBlond PH** (1966) On the damping of internal gravity waves in a continuously stratified ocean. *Journal of Fluid Mechanics* **25**(1), 121–142. doi:10.1017/S0022112066000089
- [10] Ostrovskiy LA and Soustova IA (1980) The upper mixed layer of the ocean as a sink of internal wave energy. *Oceanology* 19, 643–648.
- [11] Ostrovsky LA (2025) Interaction of hydrodynamic turbulence with stratified flows and internal waves: the role of turbulent diffusion and density fluctuations. *Physica D: Nonlinear Phenomena* 476, 134661. doi:10.1016/j.physd.2025.134661
- [12] Miles JW (1961) On the stability of heterogeneous shear flows. *Journal of Fluid Mechanics* 10(4), 496–508. doi:10.1017/ S0022112061000305
- [13] Howard LN (1961) Note on a paper of John W. Miles. Journal of Fluid Mechanics 10(4), 509–512. doi:10.1017/ S0022112061000317
- [14] Moum JN, Farmer DM, Smyth WD, Armi L and Vagle S (2003) Structure and generation of turbulence at interfaces strained by internal solitary waves propagating shoreward over the continental shelf. *Journal of Physical Oceanography* 33(10), 2093–2112. doi:10.1175/1520-0485(2003)033<2093:SAGOTA>2.0.CO;2
- [15] Forryan A, Martin AP, Srokosz MA, Popova EE, Painter SC and Renner AH (2013) A new observationally motivated Richardson number based mixing parametrization for oceanic mesoscale flow. *Journal of Geophysical Research: Oceans* 118(3), 1405–1419. doi:10.1002/jgrc.20108
- [16] Avicola GS, Moum JN, Perlin A and Levine MD (2007) Enhanced turbulence due to the superposition of internal gravity waves and a coastal upwelling jet. *Journal of Geophysical Research: Oceans* 112(C6), C06024. doi:10.1029/2006JC003831
- [17] Moum JN, Hughes KG, Shroyer EL, Smyth WD, Cherian D, Warner SJ, Bourlès B, Brandt P and Dengler M (2002) Deep cycle turbulence in Atlantic and Pacific cold tongues. *Geophysical Research Letters* 49(8), 2021GL097345. 10.1029/2021GL097345
- [18] Chang MH, Cheng YH, Yang YJ, Jan S, Ramp SR, Reeder DB, Hsieh WT, Ko DS, Davis KA, Shao HJ and Tseng RS (2021) Direct measurements reveal instabilities and turbulence within large-amplitude internal solitary waves beneath the ocean. *Comm. Earth & Environment* 2(1), 15. 10.1038/s43247-020-00083-6
- [19] Palmer MR, Stephenson GR, Inall ME, Balfour C, Düsterhus A and Green JAM (2015) Turbulence and mixing by internal waves in the Celtic Sea determined from ocean glider microstructure measurements. *Journal of Marine Systems* 144, 57–69. doi:10.1016/j.jmarsys.2014.11.005
- [20] **Ostrovsky LA and Troitskaya YI** (1987) Model of turbulent transfer and turbulence dynamics in a stratified shear flux. *Izvestiya, Atmospheric and Oceanic Physics* **23**(10), 767–772.
- [21] Ostrovsky L, Soustova I, Troitskaya Y and Gladskikh D (2024) Evolution of small-scale turbulence at large Richardson numbers. *Nonlinear Processes in Geophysics* 31(2), 219–227. doi:10.5194/npg-31-219-2024
- [22] Soustova IA, Troitskaya YI, Gladskikh DS, Mortikov EV and Sergeev DA (2020) A simple description of the turbulent transport in a stratified shear flow as applied to the description of thermohydrodynamics of inland water bodies. *Izvestiya*, Atmospheric and Oceanic Physics 56, 603–612. doi:10.1134/S0001433820060109
- [23] Gladskikh D, Ostrovsky L, Troitskaya Y, Soustova I and Mortikov E (2023) Turbulent transport in a stratified shear flow. Journal of Marine Science and Engineering 11(1), 136. doi:10.3390/jmse11010136
- [24] Ostrovsky L, Gladskikh D and Soustova I (2024) Dynamics of turbulence in the field of nonlinear internal waves. Pres. at the 23rd session of the Council of Russian Acad. Sci. (RAS) on nonlinear dynamics. Abstr on the site of Shirshov Inst of Oceanology RAS.
- [25] D'Asaro EA and Lien R-C (2000) The wave–turbulence transition for stratified flows. *Journal of Physical Oceanography* 30, 1669–1678. doi:10.1175/1520-0485(2000)030<1669:TWTTFS>2.0.CO;2

14 Ostrovsky et al.

- [26] Lewin SFA, Balakrishna A and Couchman MMP (2024) Pathways to turbulence from internal waves in a stratified horizontally sheared flow. Center for Turbulence Research Proc. Summer Program 2024, 529–538.
- [27] Rodda C et al (2023) From internal waves to turbulence in a stably stratified fluid. Physical Review Letters 131, 264101. doi:10.1103/PhysRevLett.131.264101
- [28] Matusov PA, Ostrovsky LA and Tsimring LS (1989) Intensification of small-scale turbulence by internal waves. *Acad. Sci. USSR, Doklady* 307(4), 258–261.
- [29] Galperin B and Sukoriansky S (2010) Geophysical flows with anisotropic turbulence and dispersive waves: flows with stable stratification. *Ocean Dynamics* 60, 1319–1337. doi:10.1007/s10236-010-0325-z
- [30] Druzhinin OA and Ostrovsky LA (2015) Dynamics of turbulence under the effect of stratification and internal waves, Nonlin. Nonlinear Processes in Geophysics 22, 337–348. doi:10.5194/npg-22-337-2015
- [31] Ivanov AV, Ostrovsky LA, Soustova IA and Tsimring LS (1983) Interaction of internal waves and turbulence in the ocean. Dynamics of Atmospheres and Oceans 7(4), 221–232. doi:10.1016/0377-0265(83)90006-4
- [32] Zilitinkevich SS, Elperin T, Kleeorin N, Rogachevskii I and Esau I (2013) A hierarchy of energy-and flux-budget (EFB) turbulence closure models for stably stratified geophysical flows. *Boundary-layer Meteorology* 146(3), 341–373. doi:10. 1007/s10546-012-9768-8